J. King Saud Univ., Vol. 20, *Science* (1), pp. 39-61, Riyadh (2008/1429H.)

Petrogenesis of Rare Metal-mineralized Albite Granite: An Example from the Late Neoproterozoic Jabal Tawlah, Northwestern Arabian Shield, Saudi Arabia

Talal M. Qadhi

Department of Mineral Resources and Rocks, Faculty of Earth Sciences, King Abdulaziz University, P.O. Box 80051, Jeddah 21598, Saudi Arabia

(Received 23/4/1427H.; accepted for publication 19/8/1427H.)

Abstract. The rare metal-bearing Tawlah granite pluton, in the northwestern part of the Arabian Shield is a late Neoproterozoic (607 Ma) post-collision alkaline A-type granite intrusion. It was emplaced in an island arc assemblage of metavolcano-sedimentary association. The contact between the granite and the country rocks is irregular, diffused and locally marked by silicification and abundant quartz veins, which affect both the country rocks and the granite. Two mineralogically different granite varieties were recorded in the pluton: i) quartz syenite, which occupies the central part of the granite mass and consists of microcline (up to 60%), albite, quartz and biotite in addition to minor accessory zircon, fluorite and opaques, and ii) albite granite that occupies the outer margin of the granite mass and consists of albite, quartz, microcline and abundant disseminations of accessory minerals (5-15%) represented by zircon, thorite, titanite, fluorite, apatite and many deep brown to black opaque grains. The field observations along with the replacement textural evidence strongly suggest a hydrothermal origin of the albite granite. Geochemical data along with Nd isotopes (ε_{Nd} = +4.2 – +5.9) indicate that the origin of the Tawlah granite involved partial melting of juvenile crustal source followed by fractional crystallization. There is a great chemical heterogeneity of the Tawlah granite varieties in terms of their major and trace element contents. The quartz syenite is peralkaline and shows a relatively homogenous and restricted composition with high Fe/Mg and total alkali contents, and low Ti, Mg, Ca and P. The albite granite, on the other hand, reveals a wide variation in major element composition (SiO_2 = 59.4 - 75.7%; Na_2O = 2.17 - 10.36%; K_2O = 0.15- 10.18%; Al_2O_3 = 9.16-15.64%) and ranges from peralkaline to mildly peraluminous (A/CNK = 0.8-1.15). They are distinguished by their high concentration of Ta (246-392 ppm), Nb (3281-8378 ppm), Hf (2044-3263 ppm), Zr (27693-37162 ppm), Y (4217-16948 ppm), Th (1125-2125 ppm) and HREE (e.g. Yb = 516-3326 ppm). The rare-metal enrichment in the Tawlah albite granite is largely controlled by hydrothermal fluids that post-date the intrusion of the granite mass. These metasomatic fluids caused albitization and concomitant precipitation of heavy REE and other rare metals (Nb, Ta, Zr and Y). The significant buildup in the heavy REE and the development of prominent Eu anomalies are the characteristic of sodium-metasomatized granites.

1. Introduction

Rare metal granites have been identified as those with high concentrations of normally dispersed elements such as F, Li, Rb, Cs, Sn, Ta, Nb, Zr and REE (i.e. the metallogenically specialized granites of [1]). Such granites occupy a special place in petrologic thinking because of their unique and often extreme chemical features. Two fundamentally different types of rare-metal granites exist: one peralkaline (agpaitic) and the other metaluminous to peraluminous (plumasitic or Li-F). Each type of granite has a distinctive set of trace element characteristics and associated mineral deposits. The peralkaline granites are extremely enriched in some trace elements, e.g. Zr, Nb and light REE; whereas the aluminous granites are enriched in Rb, Ta, U and Sn. In general, these granites appear to be part of the anorogenic group of granites (A-type) identified by [2, 3]. The origin of rare-metal albite-rich granites and the mechanisms of element enrichment and distribution within them have been the subject of many studies, but controversy remains about the relative roles of magmatic and hydrothermal processes (e.g. [4-9]). The central problem is that late-stage mineral replacements and zones of hydrothermal alteration are commonly observed in these granites, making it difficult to separate the effects of igneous fractionation from post-magmatic processes.

During the Neoproterozoic crustal evolution of the Arabian Shield, immense volumes of granitic rocks were emplaced. They constitute about 63% of the plutonic assemblage [10] and are subdivided into three groups, namely: 1) granodiorite and granite-granodiorite assemblage (760-660 Ma), 2) monzogranite and syenogranite (660-610 Ma), and 3) alkali feldspar granite (610-565 Ma). Geologic investigations by [11-13] have identified a group of alkali granites, defined as "metallogenically specialized granites" according to the classification of [1], which are geochemically anomalous and contain high contents of Zn, Sn, W, Rb, Nb, Ta, Y, Zr, Th, REE and other rare metals, but are depleted in Ba and Sr. At the Jabal Tawlah area, situated in the northwestern part of the Arabian Shield in Saudi Arabia (Fig. 1), tin and rare metals (Zr, Nb, Ta, Y, REE) occur within a highly evolved albite granite phase. Petrographic and mineralogical characteristics of the Jabal Tawlah albite granite, in conjunction with geochemical and isotopic data, have been used to develop a model for the evolution of the granites and the formation of the associated rare-metal mineralization.

2. Geological Setting

2.1. General geology

The studied area is a part of the Bada quadrangle (Sheet 28A, international index NF-36-16), which represents a part of the Midyan terrain between lat. 28° 00′ and 29° 00′ N and long. 34° 30′ and 36° 00′ E [14]. The main rock units exposed in the map area (Fig. 1) include: 1) Hegaf Formation, which occupies the southeastern sector of the map area and consists of metamorphosed mafic and felsic tuff, meta-andesite, metabasalt, meta-conglomerate, mica schist, and meta-siltstone as well as subordinate calc-silicate rocks and chert. This broad variation in lithology reflects depositional changes in an

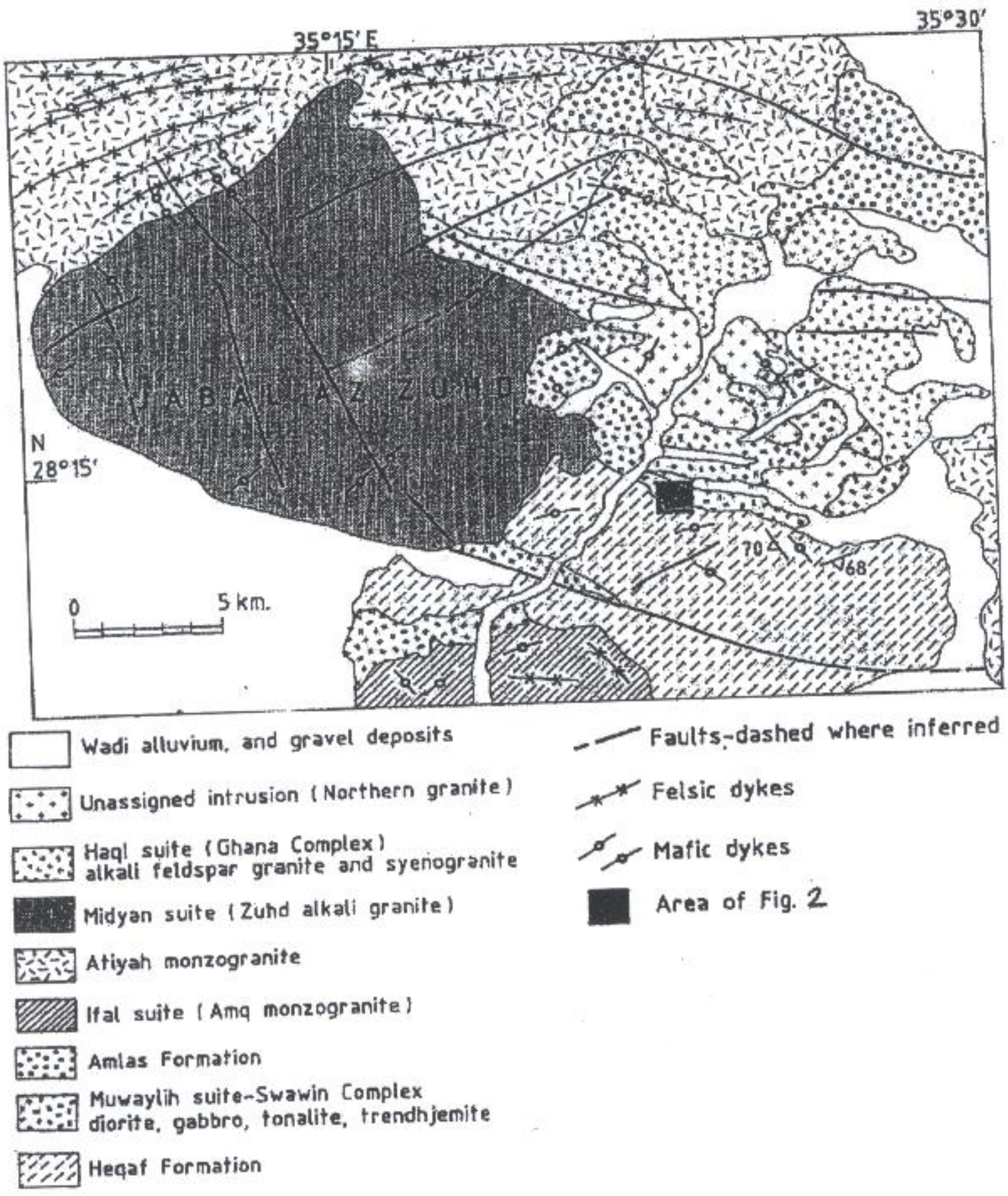

Fig. 1. Geologic map of a part of the Bada quadrangle representing the area of Jabal Az-Zuhd and location of Jabal Tawlah (Fig. 2).

island-arc environment, 2) Sawawin Complex (part of the Muwaylih suite) that consists mainly of heterogeneous medium-grained meta-diorite and quartz diorite rocks, but generally range in composition from granodiorite to gabbro, 3) Amlas Formation, which is exposed in the extreme northeastern part of the map area. It consists predominantly of conglomerate, breccia, immature sandstone, greywacke, and siltstone. The thickness of

the formation is estimated to be about 2000 m [14], 4) The Amlas Formation is intruded by monzogranite and granodiorite assigned to the Ifal suite, which are dated by U-Pb method at 625 Ma [15], and 5) Atiyah monzogranite occurs as several circular to subcircular plutons and stocks up to 15 km across. It intrudes rocks of the Ifal and Sawawin but is intruded by the Midyan and Haql alkali feldspar granites and monzogranites. The Atiyah monzogranites have been dated at 598 ± 30 Ma (Rb-Sr method) and 599 ± 5 Ma (U-Pb method) by [14].

2.2. Geologic setting of Jabal Tawlah

The granitic body of Jabal Tawlah occurs as an irregular elongated body (400 × 200 m) that occupies the SE part of the map area (Fig. 1). It intrudes the volcano-sedimentary rocks of the Hegaf Formation and lies at about 5 km from the eastern margin of Jabal Az-Zuhd alkali feldspar granite pluton. The contacts between this granitic body and the country rocks are irregular, diffused and locally marked by silicification and abundant quartz veins (Fig. 2). The northeastern contact is partly faulted or controlled by pre-existing fault. The lower part of the granitic body shows a marked intermixed and amalgamated relation with its country rocks, but appears as massive white granite at the top of the ridge. Silicification and abundant divergent quartz veins and pods are common. Also, irregular white granitic patches are randomly distributed in the country rocks of Jabal Tawlah. Many granitic patches and veinlets, similar in composition and mineralogy to the Jabal Tawlah granite, are recorded in the volcanosedimentary rocks in another location about 1 km southwest of Jabal Tawlah.

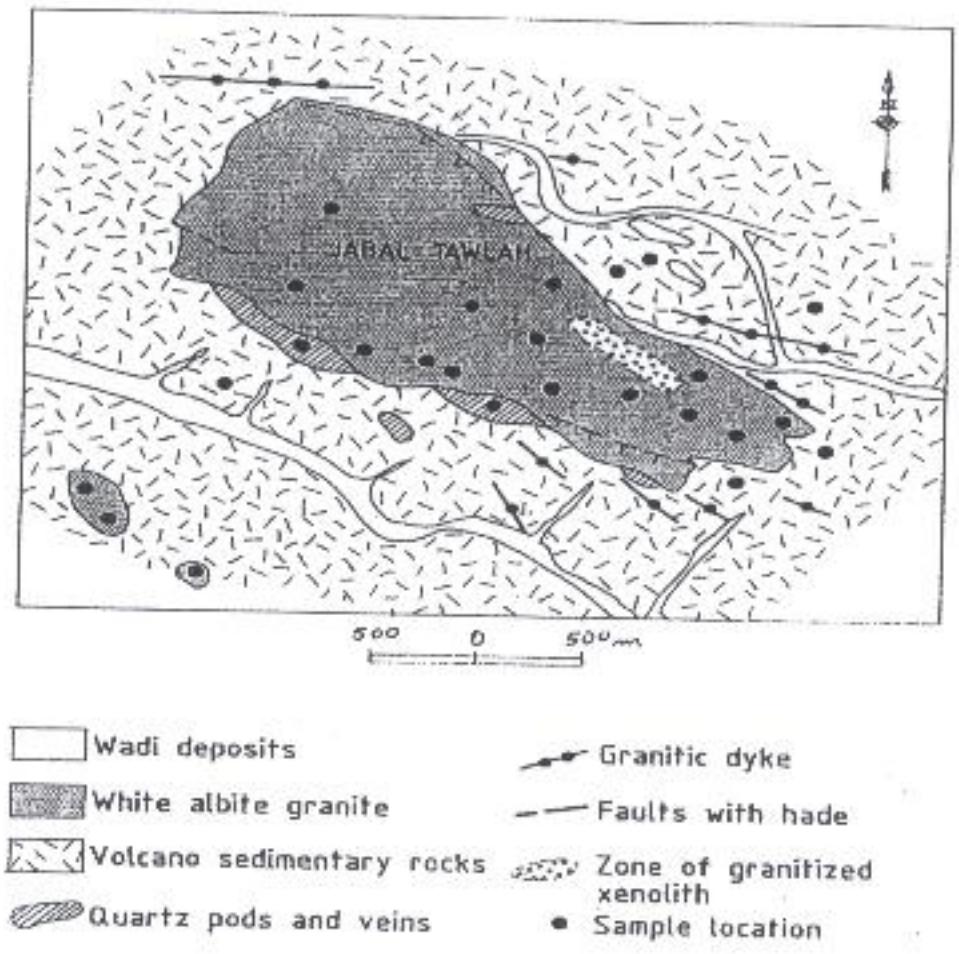

Fig. 2. Simplified geologic map of Jabal Tawlah showing the location of the collected samples.

In spite of the small size of the Jabal Tawlah granite, the rocks show great variation in the proportion of their mineral constituents, textural relationship, abundance and nature of accessory minerals and degree of deformation. The rocks are generally ineqigranular, locally foliated, fine- to medium-grained with grayish white to vivid white colors but tend to be of yellowish to reddish white color in the more altered samples. Cataclasis due to intense brecciation and deformation and later silicification are locally well developed, particularly near their contacts with the host volcano-sedimentary rocks. Regarding mineralization and ore minerals encountered in the Jabal Tawlah, a major part of Th, Y, Zr , Nb, Ta and REE-bearing accessory minerals are frequently abundant as dissemination and may reach in some samples up to 15% of the rock mode. In addition, irregular black patches and veinlets with submetallic luster are recorded in the Jabal Tawlah granite. These black patches are similar to those found in many Nb-Ta-bearing albite granite (apogranite) in Abu Dabbab, Niewbi, Homrt Waggat, Egypt [16, 17].

Based on the above-mentioned features, the rocks of Jabal Tawlah can be broadly grouped into medium-grained albite granite, quartz syenite and porphyritic albite cataclastic granite (cataclasites). Field radiometric invesitigation of the three rock units and the country rocks gave the following results: 1) The medium-grained albite granite is the main rock type in the Jabal Tawlah which gave high radioactive readings ranging from 1800 cps to 2300 cps with an average value of about 1900 cps; 2) The quartz syenite follows the medium-grained albite granite in abundance and possesses relatively lower radioactivity commonly in the range from 1000 cps o 1400 cps; 3) The porphyritic cataclastic albite granite is characterized by strong shearing and silicification and yielded the highest gamma field radioactivity which reachs up to 3200 cps with an average value of about 2500 cps; 4) Shear zones and some quartz veins gave also high radioactive readings commonly in the range of 1900 cps to 2500 cps; 4) The volcano-sedimentary rocks and the dykes have the lowest radioactivity with an average value of 70 cps to 50 cps; Silicified and bleached zones in the country rocks (volcano-sedimentary rocks) close to the granites show variable but relatively high radioactivity ranging from 200 cps to 1000 cps.

3. Petrography

Jabal Tawlah albite granite constitutes the main part of the Jabal Tawlah granite. The rocks are medium-grained, hypidiomorphic, with different shades of whitish color. The medium-grained albite granite consists of albite, quartz and microcline. Accessory and opaque minerals are relatively abundant forming about 5 to 15% of the rock mode. Albite ($Ab_{90} - Ab_{95}$) is the dominant mineral with an average 45% of the rock mode. The albite crystals are medium- to fine-grained, subhedral and prismatic to lath-like. The albite laths exhibit interpenetrating and interlocking textures, while in other samples they display subparallel alignment around the elongated and deformed coarse-grained quartz and microcline crystals. The black patches found in some rock samples represent actually cluster aggregates of albite laths that are delineated with black to deep brown materials mostly of iron oxides. Quartz follows albite in abundance forming about 25 to

30% of the rock mode. The quartz crystals are medium-grained, anhedral and highly strained with the development of strong undulose extinction. Poikilitic inclusions of albite and microcline crystals in quartz are common. Microcline is present as fine grains of subhedral to anhedral form. Zircon, thorite, titanite, fluorite, apatite and many deep brown to black grains (opaques) are frequently abundant. They are sporadically scattered in the rock, but in some rock samples are clustered in aggregates. Thorite is the most abundant accessory mineral in the rock. The crystals of thorite are subhedral to anhedral with inclusions of very fine albite laths and iron oxides. Many crystals of thorite are partially mitamictized and covered with amorphous blackish brown materials. Zircon follows thorite in abundance and occurs as minute colorless and clear crystals with subhedral to anhedral form. Fluorite occurs as large anhedral crystals with irregular form. Some crystals of fluorite contain relict inclusions of feldspar.

The *J. Tawlah quartz syenite* is of limited distribution and occurs in the southeast and extreme northwest of Jabal Tawlah granite occupying the central part of the pluton. It consists of microcline, quartz and subordinate albite and biotite. Some rock samples are foliated, slightly deformed and affected by silicification. Microcline crystals constitute about 60% of the rock mode. They are fine-grained but few large phenocrysts are common forming cluster aggregates. Quartz crystals are fine-grained with anhedral granular and amoeba-like form. They are generally strained with severe undulose extinction. Relatively large crystals contain abundant inclusions of microcline. Albite crystals are fine to medium-grained, subhedral with prismatic to lath-like shape. Some medium-grained albite crystals show "chessboard" structure [18]. The texture reflects a low temperature structural state of the feldspar due perhaps to subsolidus modification. Biotite is present as fine-grained flakes of pale brown color. Most of the biotite flakes occur in vein-like form or filling fracture. Accessory minerals in the quartz microsyenite are less abundant than the fine-grained albite granite and include thorite, zircon, fluorite and abundant opaque minerals.

Jabal Az-Zuhd consists of two main rock types. These are aegirine-arfvedsonite alkali granite and alkali feldspar granite. The aegirine-arfvedsonite alkali granite is hypersolvous, coarse- to very coarse-grained with an average grain size of about 8 mm. It is equigranular hypidiomorphic with grayish white, greenish gray to pale pink color and consists of microcline, microcline microperthite, quartz, aegirine and arfvedsonite. Accessory minerals include zircon, rutile and allanite. K-feldspar includes microcline and microcline micro-to cryptoperthite. The K-feldspar crystals are coarse-grained and of subhedral to anhedral form, constituting 60 to 70% of the rock mode. Quartz crystals are coarse grained, anhedral and slightly deformed. Alkali pyroboles include aegirine, arfvedsonite and minor riebeckite. Aegirine crystals of olive-green color are fine-grained and weakly pleochroic. Some crystals are partly replaced by arfvedsonite with relicts of aegirine retained in the core of the coarse arfvedsonite crystals.

The *northern granite* is a subsolvus monzogranite that represents the main rock type in the pluton. The rock consists of rather equal proportions of quartz, plagioclase

feldspar, K-feldspar (micro- and mesoperthites) and minor biotite. Zircon, apatite and iron oxides are the common accessory minerals. Secondary alteration minerals include chlorite, sericite, calcite, iron oxides and clayey minerals.

4. Geochemistry

4.1. Sampling and analytical techniques

Based on the petrographic investigations, 19 representative samples covering the different granite varieties were selected for major and trace element analyses. Major element compositions and Sc, Ba and Ni abundances were determined by inductively coupled plasma-atomic emission spectrometry (ICP-AES). The remainder of trace elements and the rare earth elements (REE) were determined by inductively coupled plasma-mass spectrometry (ICP-MS). All the analyses were carried out at the ACME Analytical Laboratories Ltd., Canada. Analytical precision, as calculated from replicate analyses, is 0.5% for major elements and varies from 2-5% for trace elements of >80 ppm, 2-10% for trace elements of 10-80 ppm, and 5-20% for trace elements of <10 ppm.

Isotopic ratios of Sr and Nd and the concentrations of Rb, Sr, Sm and Nd were determined by isotopic dilution analysis, except samples with high concentration of Rb and Sr were determined by X-ray fluorescence (XRF). The analyses were determined at the Geology Department, Bergen University, Norway using a VG 354 and Finnigan MAT 262 mass spectrometer. The $^{87}Sr/^{86}Sr$ and the $^{143}Nd/^{144}Nd$ ratios were normalized within runs to $^{87}Sr/^{86}$ Sr = 0.1194 and to $^{146}Nd/^{144}Nd$ = 0.7219. Laboratory values for standards at the time of running the samples were: Johanson and Matthey (JM) Nd_2O_3, batch No. S819093A yielded $^{143}Nd/^{144}Nd = 0.511101 \pm 15$ (2 σ); NBS 987 yielded $^{87}Sr/^{86}$ Sr = 0.71015 ± 0.00004 (2 σ, mean). The laboratory total system blank were generally < 1 ng for Sr and Nd. Initial $^{143}Nd/^{144}Nd$ and $^{87}Sr/^{86}$ Sr were calculated for individual samples at the time of crystallization and are expressed in ϵ^t_{Nd} and ϵ^t_{Sr} using present-day $^{147}Sm/^{144}Nd$ = 0.1967; $^{143}Nd/^{144}Nd$ = 0.512638; $^{87}Rb/^{86}$ Sr = 0.0827 and $^{87}Sr/^{86}Sr$ = 0.7045 [19, 20]. The decay constant (I) used for ^{147}Sm is 6.54 10^{-12} y^{-1} and for 87Rb is 1.42 x 10^{-11} y^{-1} [21]. Model Nd ages (T_{DM}) were calculated according to the depleted mantle model of [22].

4.2. Major and trace element variations

Major and trace element analyses of Jabal Tawlah granite are presented in Table 1. Analyses of the nearby granites are also included for comparison — three samples from Az-Zuhd alkali feldspar granite and two analyses from the northern granite. The albite granite of Jabal Tawlah reveals a wide variation in major element composition (SiO_2 = 56.4 - 75.7%; Na_2O = 2.17 - 10.36%; K_2O = 0.15- 10.18%; Al_2O_3 = 9.16-15.64%). The quartz syenite, on the other hand, shows a more homogenous and restricted composition than the albite granite. In addition, all the specimens have high Fe/Mg and total alkali contents, and low Ti, Mg, Ca and P. Most of the major element variation diagrams (Fig. 3) show a rather scatter with no definite trend. The major elements discrepancies leave their signature on the albite granite. The rocks of the albite granite have a wide A/CNK molar ratio (0.8-1.15) and A/NK (0.9-1.1), and on Shand diagram [23] they

Table 1. Major and trace elements data of Jabal Tawlah and Jabal Az Zuhd granites

	Jabal Tawlah											Jabal Az Zuhd and Northern granite				
	Albite granite							Quartz microsyenite				Alkali feldspar granite				
	T-2	T-6	T-7	T-8	T-45	T-46	T-36B	T-2B	T-34	T-40	T-48	Z-2	Z-3	Z-4	NG-2	NG-4
SiO_2	63.84	75.70	74.52	75.17	56.31	59.44	74.04	77.58	67.82	73.40	74.36	70.29	78.39	77.06	74.78	73.19
TiO_2	0.54	0.81	0.75	0.66	3.30	1.28	0.98	0.05	0.11	0.23	0.06	0.08	0.18	0.15	0.12	0.11
Al_2O_3	15.64	9.60	9.55	9.98	15.03	15.26	9.16	11.78	16.64	11.41	12.75	10.62	10.09	10.60	12.46	12.5
Fe_2O_3	1.18	0.93	1.63	1.81	3.24	1.59	1.24	0.85	1.13	2.79	1.36	1.68	2.70	2.42	1.19	1.27
MnO	0.09	0.06	0.06	0.04	0.29	0.11	0.11	0.01	0.01	0.08	0.01	0.08	0.04	0.03	0.02	0.03
MgO	0.07	0.01	0.11	0.04	0.01	0.10	0.06	0.13	0.27	0.88	0.04	0.01	0.48	0.03	0.27	0.23
CaO	0.42	0.29	0.24	0.14	0.63	1.06	0.23	0.39	0.78	1.10	0.38	4.77	0.53	0.17	0.84	1.26
Na_2O	8.35	4.15	5.07	3.87	10.36	2.17	3.57	6.27	11.29	7.46	4.78	5.33	6.24	3.52	3.03	4.31
K_2O	2.14	1.67	1.33	1.90	0.15	10.18	2.34	2.05	0.34	0.55	5.43	2.50	1.25	4.49	4.54	4.58
P_2O_5	0.02	0.01	0.02	0.01	0.64	0.02	0.02	0.04	0.01	0.01	0.01	0.02	0.01	0.01	0.01	0.03
LOI	1.20	1.00	1.00	1.00	1.30	1.90	1.60	0.50	0.80	1.60	0.60	2.50	0.20	0.30	1.2	1.3
Sum	93.49	94.23	94.28	94.62	91.26	93.11	93.35	99.65	99.20	99.51	99.78	97.88	100.1	98.78	98.46	98.81
Ni	3	2	3	2	1	4	7	2	4	7	1	8	4	8	4	6
Co	39	1	5	1	1	3	2	8	2	6	3	1	8	2	2	3
Sc	7	4	4	4	18	10	5	2	2	3	1	1	1	1	2	3
V	3	3	3	3	3	5	3	3	6	23	3	3	9	3	8	6
Cu	17	13	30	53	20	20	175	4	3	62	9	41	8	3	17	7
Pb	214	263	462	1023	160	103	1615	21	89	45	8	891	4	9	8	28
Zn	1431	2457	1404	2209	594	2290	6063	71	252	1540	449	760	50	264	23	19
Sn	931	808	486	1057	51	33	731	6	13	83	10	233	6	12	1	1
W	793	12	127	33	25	53	72	197	49	35	73	3	87	120	1	119
Rb	279	177	224	321	32	825	386	132	102	198	252	1032	18	110	130	158
Cs	1.40	1.00	1.10	1.60	0.30	2.50	2.00	0.50	2.10	3.10	0.60	3.30	0.10	0.50	2	7.1

Table 1 *(Contd.)*

	Jabal Tawlah											Jabal Az Zubd and Northern granite				
	Albite granite							Quartz microsyenite				Alkali feldspar granite				
	T-2	T-6	T-7	T-8	T-45	T-46	T-36B	T-2B	T-34	T-40	T-48	Z-2	Z-3	Z-4	NG-2	NG-4
Ba	508	70	127	132	32	171	415	66	17	43	26	15	170	67	532	471
Sr	139	91	82	36	129	168	22	29	80	97	12	47	62	13	116	117
Ga	102	88	100	95	93	89	86	44	59	45	48	64	23	35	15	18
Ta	339	312	246	270	392	334	261	10.1	25.7	15.7	15.0	115	5.4	8.0	1.5	2.8
Nb	4471	3923	3281	3657	8378	5576	3435	174	404.3	221.3	205.7	1143	46.2	97.5	10.6	15.8
Hf	2044	2058	2404	2120	3263	2453	2876	28	38.8	42.8	15.5	377	13.8	30.3	3.8	3.9
Zr	32212	31936	37144	30924	37162	30903	27693	572	872	805	326	7386	494	1101	94	97
Y	6653	4453	4217	3745	16948	12016	9733	220	536	564	198	800	62	183	19	23
Th	1212	1187	2003	1654	1125	2125	1823	11.9	22.8	22.7	11.9	238.8	7.1	14.5	12.9	17
U	4.20	3.60	3.30	2.80	25.40	40.30	1.40	5.30	8.10	6.10	5.10	113	1.80	5.40	3.8	5
La	7.60	2.80	1.90	1.90	7.40	39.10	2.90	20.70	39.90	24.80	10.10	30.10	52.30	65.70	19.5	29
Ce	19.50	7.50	5.60	6.10	38.30	147.1	6.70	62.60	107.9	74.30	36.40	98.20	123.2	163.9	37	56.3
Pr	3.10	0.70	0.80	0.80	6.20	18.20	1.20	9.20	15.20	9.40	4.30	9.24	14.87	21.78	4.09	6.13
Nd	12.20	3.60	3.80	3.30	23.20	67.80	6.40	44.50	67.40	43.60	20.80	24.90	60.10	92.60	14.8	21.3
Sm	17.60	8.50	8.30	7.80	32.90	56.90	11.50	16.90	23.30	15.70	8.80	12.10	14.03	23.10	3.4	4.1
Eu	1.10	0.80	0.80	0.90	5.20	4.00	0.90	0.60	0.80	0.90	0.30	0.27	2.07	3.27	0.44	0.48
Gd	96.8	50.4	46.5	46.2	177.6	2012	75.4	23.70	29.40	21.30	15.10	18.29	12.75	27.84	2.44	3.67
Tb	68.1	38.7	36.3	40.5	153.7	116.5	63.9	4.50	6.20	5.10	3.50	9.16	1.98	4.69	0.47	0.62
Dy	796.8	477.6	469.4	564.8	2232	1293	887.6	35.30	53.40	47.00	28.30	107.1	12.78	30.91	3.11	4.07
Ho	218.1	138.8	151.4	183.9	706.7	654.3	280.7	8.00	14.70	14.50	7.30	33.83	2.47	6.60	0.63	0.78
Er	742.4	487.6	618.0	785.2	2890	1235	1145	23.50	56.10	60.30	22.50	160.8	7.33	18.86	1.99	2.39
Tm	118.0	82.8	118.9	165.9	538.1	196.2	218.6	2.80	10.10	12.40	2.90	35.39	1.06	2.56	0.27	0.38
Yb	694.6	515.5	791.2	1097	3326	1085	1398	18.50	87.80	106.4	19.2	290.1	7.37	17.32	2.37	2.78
Lu	95.0	74.3	110.9	145.0	421.2	139.9	187.4	2.20	12.80	15.30	2.40	45.09	1.15	2.69	0.34	0.45

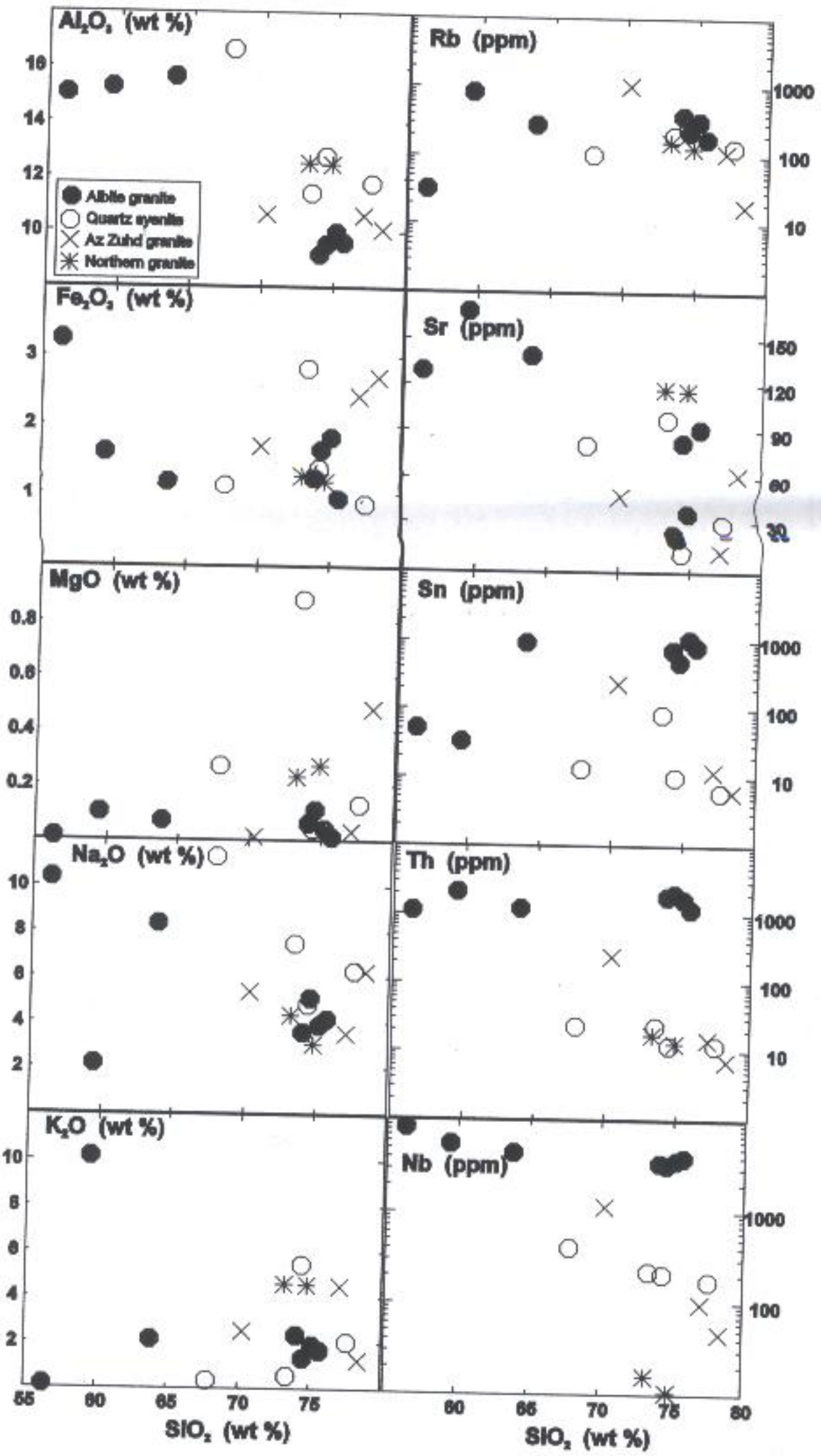

Fig. 3. Harker variation diagrams of some major and trace elements of the Jabal Tawlab, Jabal Az-Zuhd and northern granites.

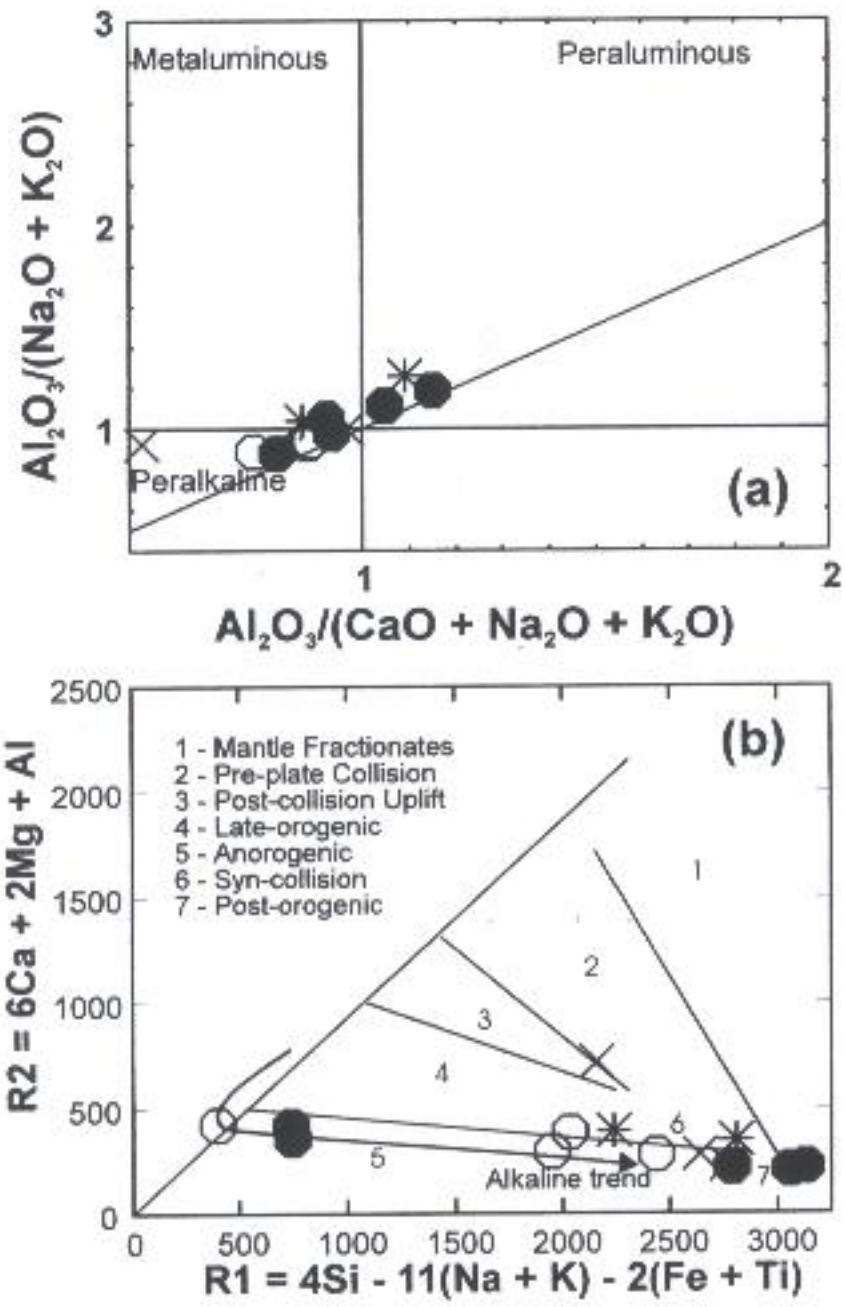

Fig. 4. (a) A plot of Shand index (A/CNK vs. A/NK) for the studied granitoids; discrimination fields are from [25], (b) R1-R2 diagram [24] with the alkaline trend from [26]. Symbols as in Fig. 3.

range from peralkaline to metaluminous and mildly peraluminous character (Fig. 4a). The quartz syenite and Az-Zuhd granites are of peralkaline character. The alkalinity of the rocks in relation to their tectonic setting is shown on the R1-R2 diagram [24]. Although all the rocks (albite granite, quartz syenite of Jabal Tawlah and the alkali feldspar granite and aegirine riebeckite granite of Jabal Az-Zuhd) follow the alkaline trend (Fig. 4b), they have large R1 values (R1 = 250-3100). The Tawlah quartz syenite samples plot in the anorogenic field, while the Az-Zuhd granites and some albite granite straddle the anorogenic and post-orogenic fields.

Concentrations of a wide variety of trace elements are shown in Table 1. The trace element compositions of the specimens from the Tawlah granite define two geochemical groups, especially on the diagrams which involve incompatible high field strength elements (Fig. 3), and indicate that the pluton is chemically zoned. The two groups produce different arrays on the plots of two elements. The albite granite is distinctive because of its high concentrations of some incompatible trace elements. Rubidium contents range from less than 200 ppm to nearly 1000 ppm. Likewise, the albite granite

is enriched relative to the quartz syenite and the nearby Az-Zuhd and northern granites in Y, Nb, Ta, Zr, Hf, Sn, U and Th. Light rare earth element (LREE) concentrations are similar to those in many other silicic rocks, but heavy REE (HREE) contents are strongly elevated. Elements concentrated in feldspars (Sr, Ba, Eu) and mafic silicates (Co, Cr) are strongly depleted. On the mantle normalized trace element diagrams (Fig. 5), trace element concentrations show complex and wide variation in the Tawlah albite rocks compared with the other alkaline granites. The quartz syenite shows more regular variation patterns with element enrichment and depletion similar to many rare-metal bearing types of granite. The albite granite of Jabal Tawlah shows marked enrichment in HFS elements (Zr, Hf, Nb, Ta, Y and HREE) and some LIL elements (Rb, Cs, Th, U) and depletion in K, Ba, Sr, Ti and LREE.

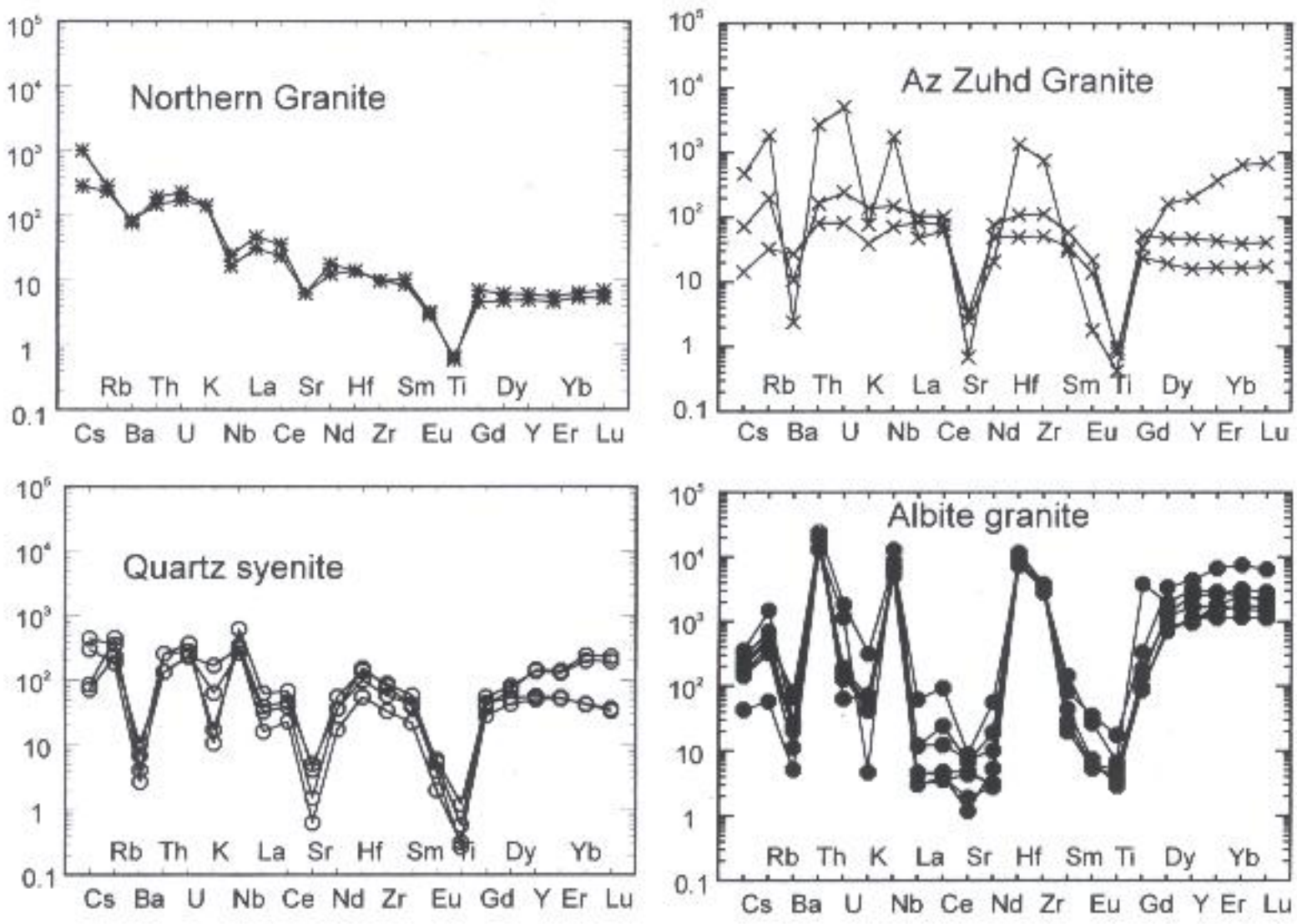

Fig. 5. Primitive mantle-normalized multi-element diagrams for the investigated granites. Normalizing values are from [27].

The REE patterns of specimens from the different granite varieties in the area are subtly distinct (Fig. 6). The alkali feldspar granite of Jabal Az-Zuhd show moderate fractionated REE patterns (La/Yb_n = 2.5-4.6; La/Sm_n = 1.7-2.2) and negative Eu anomalies (Eu/Eu* = 0.4-0.5). One sample (aegirine arfvedsonite peralkaline granite) is characterized by HREE enrichment (Gd/Yb_n = 0.08) and stronger negative Eu anomaly (Eu/Eu* = 0.07). The northern granites have more fractionated LREE pattern (La/Yb_n = 5.3-6.8) and smaller Eu anomaly than Az-Zuhd granites. The Jabal Tawlah quartz

syenite show positive fractionated REE (La/Yb_n = 0.2-0.7, Gd/Yb_n = 0.3-1.6), flat LREE (La/Sm_n = 0.96-1.57) and strong negative Eu anomalies (Eu/Eu* = 0.09-0.15). The albite granite shows characteristic REE pattern with flat and variable LREE enrichment (La/Sm_n = 0.13-0.99), strong positive HREE fractionation (Gd/Ybn = 0.05-2.3) and moderate negative Eu anomalies (Eu/Eu* = 0.04-0.21). Unlike the quartz syenite, the albite granites have extreme REE enrichment (Σ REE = 1890-10559 ppm) compared with the quartz syenite (Σ REE = 182-525 ppm). This type of HREE enrichment in the albite granite, which is 10 to 15 times that of the quartz syenite, is difficult to explain by normal fractional crystallization.

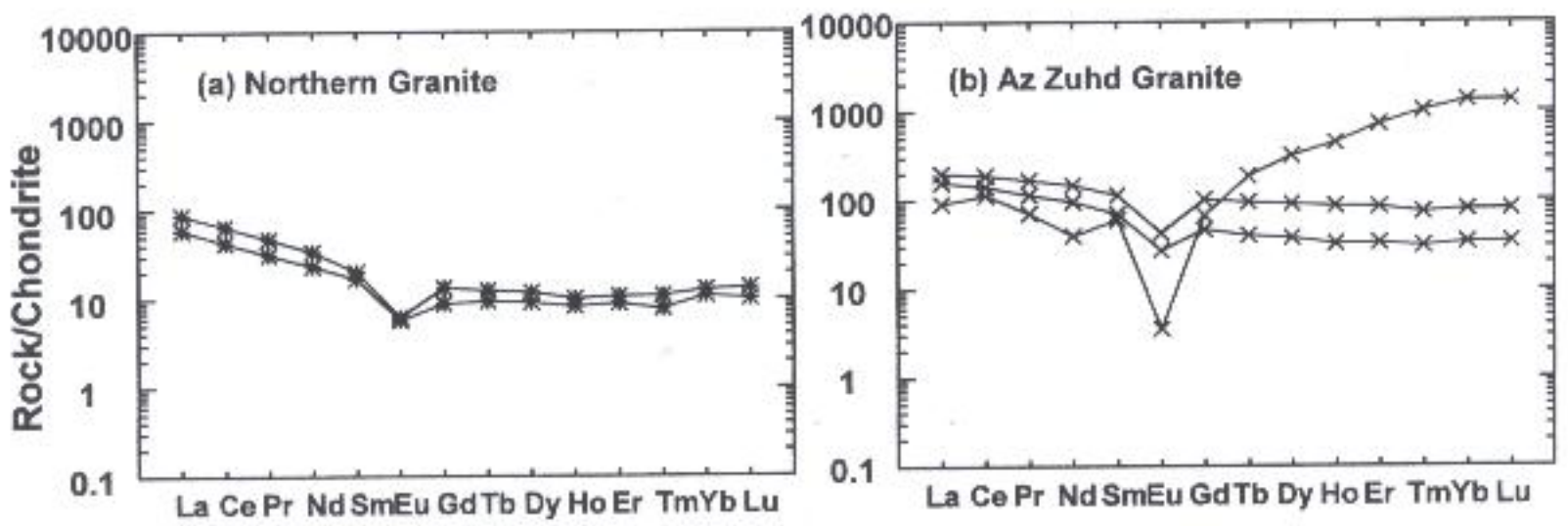

Fig. 6. Chondrite-normalized REE patterns of the investigated granites. Normalizing values are from [28].

4.3. Sr and Nd isotopes

Five samples of the albite granite from Jabal Tawlah were analyzed for Rb-Sr and Sm-Nd isotope and the whole rock analytical data are given in Table 2. Regression of the Sr isotopic data presented in Table 2 yield an age of 636 ± 74 Ma and an initial $^{87}Sr/^{86}Sr$ ratio of 0.7008 ±14, MSWD = 88 (Fig. 7a). The large errors in the age and intercept probably reflect variable wall rock interaction as a result of variation of the fluid chemistry and/or composition of the wall rock. The Sm-Nd isotopic analyses of four samples presented in Table 2 are plotted in Fig. 7b. The four analytical points define a good linear correlation (MSWD = 0.87) when plotted on the $^{143}Nd/^{144}Nd$ versus $^{147}Sm/^{144}Nd$ isochron diagram. The slope of this isochron corresponds to an age of 607 ±

14 Ma. This age appears to reflect either the time of intrusion of the granite or it may reflect the age of hydrothermal alteration. The initial $^{143}Nd/^{144}Nd$ ratios, as represented by ε_{Nd}, vary between +4.2 and +5.9, which indicate that the studied rocks were derived from a juvenile source, and preclude the presence of old continental crust in the study area.

Table 2. Rb-Sr and Sm-Nd data for the Jabal Tawlah granite

Sample No.	$^{87}Rb/^{86}Sr$	$^{87}Sr/^{86}Sr$ (± 2σ)	$^{147}Sm/^{144}Nd$	$^{143}Nd/^{144}Nd$(± 2σ)	ε^{t}_{Nd}	T_{DM} (GA)
T-4	1.16	0.710406 ± 10	0.133	0.512611 ± 15	4.24	0.74
T-8	24.75	0.929083 ± 9	1.560	0.518315 ± 9	4.78	0.60
T-34	4.03	0.738037 ± 9	0.215	0.513008 ± 6	5.62	0.67
T-45	0.88	0.708652 ± 9	0.791	0.515315 ± 6	5.93	0.61
T-47	0.26	0.703992 ± 10				

The 2σ standard error in $^{87}Rb/^{86}Sr$ and $^{147}Sm/^{144}Nd$ is 1%. Analytical uncertainties in $^{87}Sr/^{86}Sr$ used to weigh the regression and calculate the MSWD are 0.2%

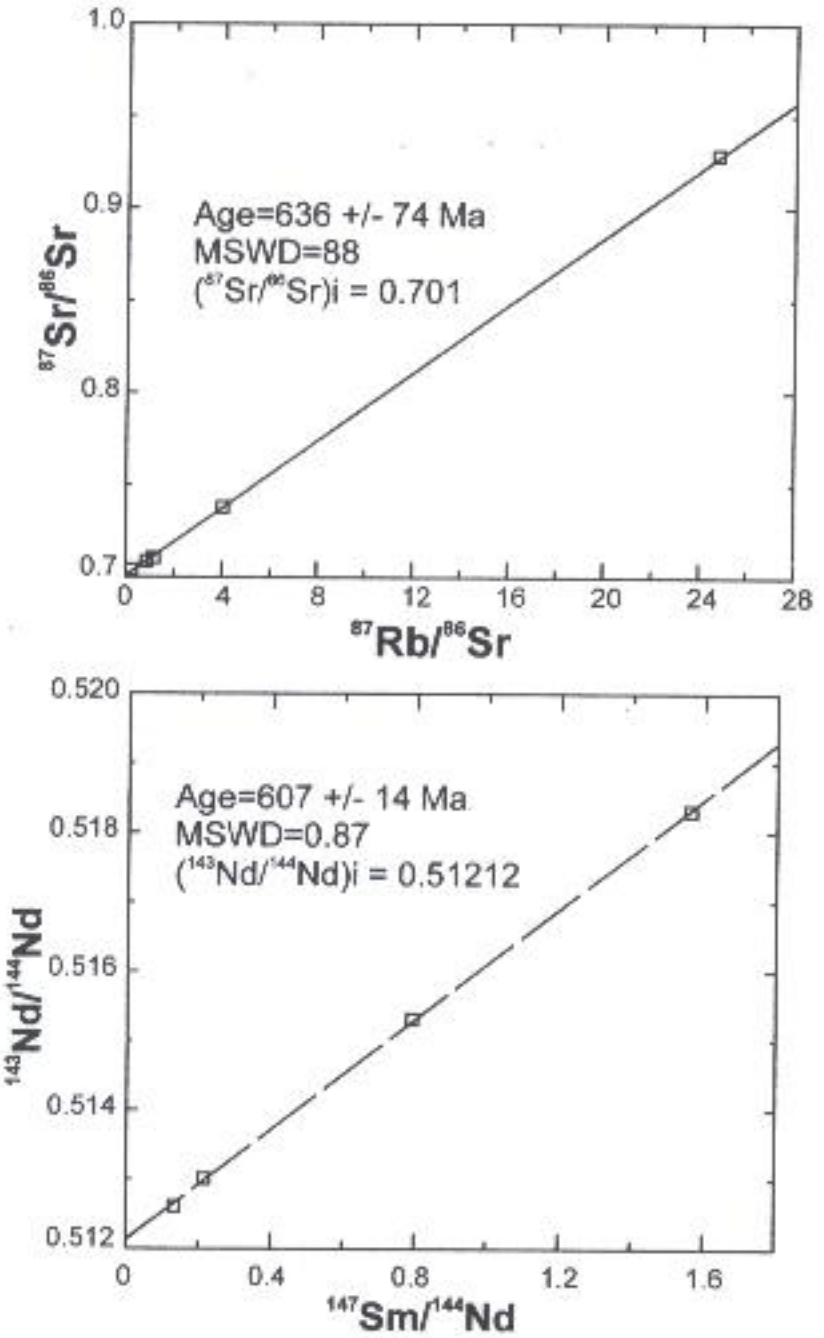

Fig. 7. Rb-Sr and Sm-Nd whole rock isochrones of the Jabal Tawlah albite granite.

5. Discussion

5.1. Petrogenesis of the Tawlah granite

The mineralogical composition and the overall chemical characteristics of Jabal Tawlah, Jabal Az-Zuhd and the northern granite (e.g. depletion of Ca, Mg and Sr and high FeO*/MgO, $(Na_2O+K_2O)/CaO$ and Ga/Al with marked enrichment in HFS elements) are consistent with the characteristics of A-type granitoids [29-32]. However, one of the most striking features of Jabal Tawlah granite is the great chemical heterogeneity in terms of their major and trace element contents, particularly as demonstrated in the albite granite. This chemical heterogeneity is consistent with the field and petrographic observations, which define the role of hydrothermal fluids in the genesis of the albite granite.

To test the role of magmatic process or the post-magmatic modification (metasomatism), the normative composition of the investigated rocks are plotted in the Q, Ab, Or haplogranite system (Fig. 8). Experimentally, the locations of the minimum melt composition, in the presence of 0, 1, 2 and 4 wt.% fluorine at 1 kbar H_2O are indicated [33]. The northern granite, Az-Zuhd and the quartz syenite of Jabal Tawlah plot close to the minimum composition in the presence of 0, 1, 2 and 4 wt.% fluorine. The albite granite of Jabal Tawlah shows a rather scatter and cannot be correlated with the pseudoternary minima of the haplogranite $-H_2O$-F system (Fig. 8). For this reason, we use here the quartz syenite (less affected by metasomatism) to discriminate the tectonic setting of the Jabal Tawlah granite. On the Nb versus Y diagram (Figs 9a), which has been devised to discriminate between granites from different tectonic settings [34], the Jabal Az-Zuhd and Tawlah granites plot in the within-plate granite field. The northern granite, on the other hand, plot in the volcanic arc field. Using diagrams for A-type granite discrimination [29], the Jabal Tawlah quartz syenite is mainly classified as A-type granite.

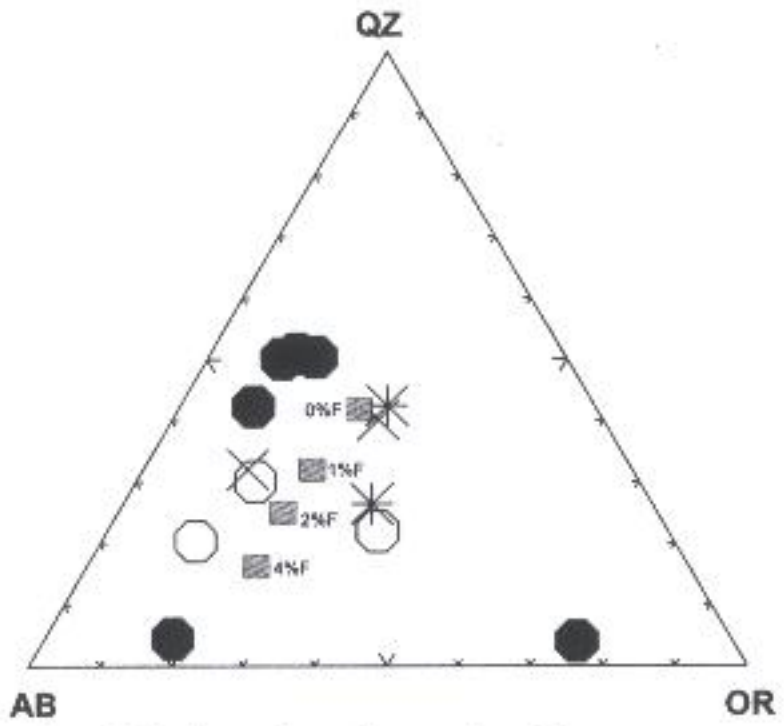

Fig. 8. Normative Q-Ab-Or plot of the investigated granites. Grey squares are minimum normative composition for the haplogranite system with 0, 1, 2 and 4% added fluorine at 1 kbar [33]. Symbols as in Fig. 3.

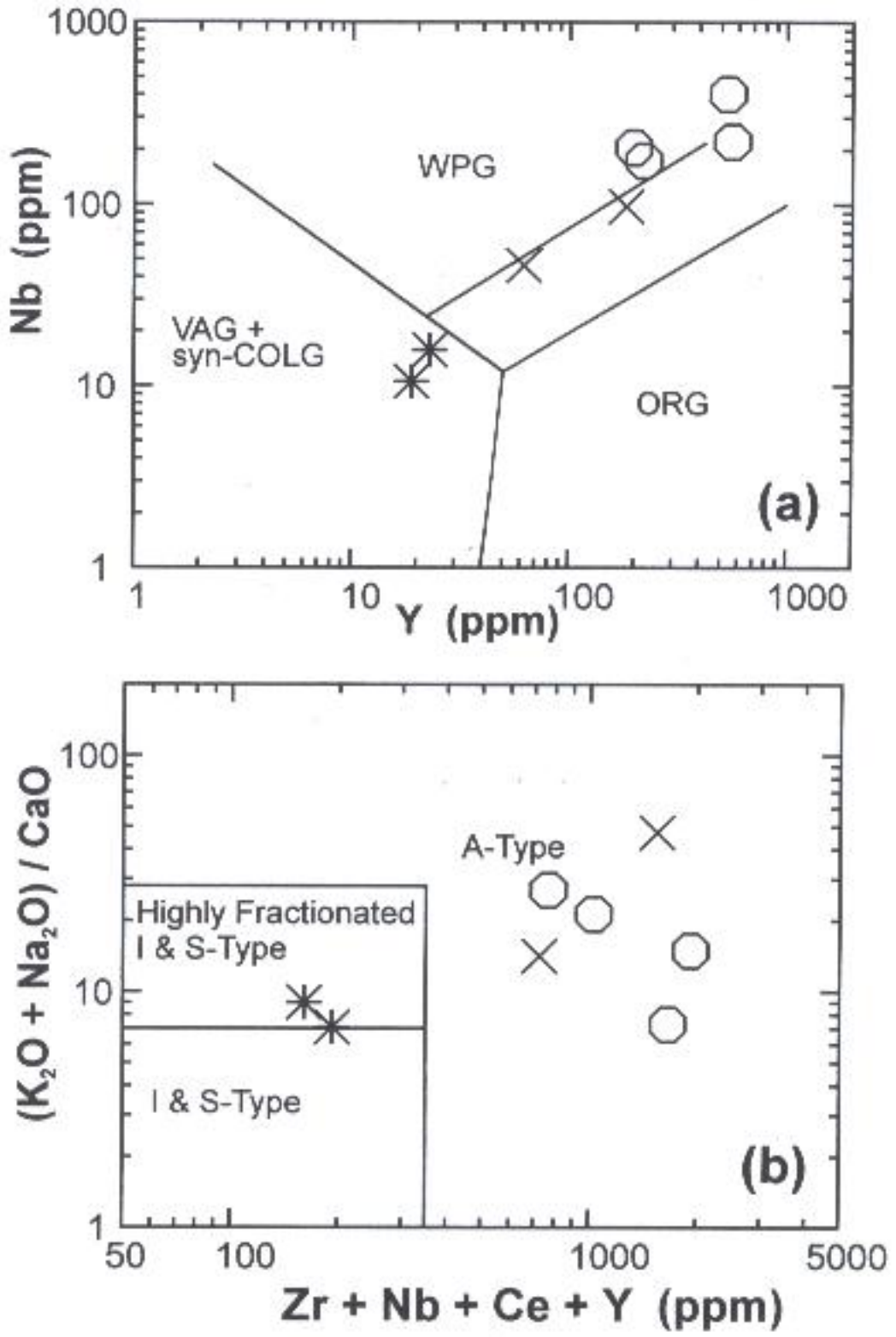

Fig. 9. Tectonic discrimination diagrams for the investigated granites. (a) Y vs. Nb diagram [34], VAG = volcanic arc granite, syn-COLG = syn-collision granite, ORG = ocean ridge granite, WPG = within plate granite; (b) $(K_2O+Na_2O)/CaO$ vs. Zr+Nb+Ce+Y discrimination diagram [29]. Symbols as in Fig. 3.

Some compositional variations observed in the quartz syenite are compatible with the partitioning of elements between a silicic melt and minerals crystallizing from that melt (e.g. fractionation of plagioclase, alkali feldspar and biotite). Their major and trace element composition defines nearly systematic variation trends on variation diagrams (Fig. 3). Also, the REE patterns and the multi-element spider-diagrams (Figs. 4a,b) display negative Eu, Sr, Ba, Ti and P anomalies, which indicate fractionation of feldspars, mica, Fe-Ti oxides and apatite. In recent years, four models have been proposed for the origin of A-type granites, namely: 1) partial melting of lower crust followed by fractional crystallization [35-37], 2) fractional crystallization of mantle-

derived mafic magma [38-40], 3) contamination of mafic mantle-derived melt by lower crustal components [41], and 4) mixing of crustal-derived and mantle-derived melts in the lower crust [42]. In the studied area, there is little evidence in favor of extensive wall-rock assimilation and magma-mixing as responsible for the chemical variations observed in the studied granites. Also, the absence of mafic rocks, of the same age as the investigated granites, precludes their direct fractionation of basaltic magma. Thus, the magma source of the investigated post-collision A-type granites is most probably a crustal source. The lower crust in the Arabian-Nubian Shield is juvenile (700 - 900 Ma) and composed of mafic layer of modified oceanic crust and mafic cumulates [43, 44]. These rocks are attractive sources to produce tonalitic melts with low SiO_2 content (52 - 55%) at lower crustal pressures [45, 46]. Thus, it is possible that the studied A-type granites could have been derived from tonalitic magma by fractional crystallization.

5.2. Origin of the rare metal mineralization

Many workers suggested that the REE enrichment in anorogenic alkaline and peralkaline granites are largely due to fluid and volatile transfer associated with alkali metasomatism [47, 48]. The Tawlah albite granites show selective enrichment of HREE over the LREE (Gd/Ybn < 1) in contrast to the behavior of REE in most alkaline and peralkaline granites. This feature suggests that other processes may control the abundance of REE and their behavior in Tawlah. The lack of experimental data, concerning the partition coefficient of REE between the hydrothermal solutions and minerals either during precipitation or interaction with source [49], put some constraint on the evaluation of the behavior of REE in hydrothermal system. Melt/vapor experiments have shown that REE do not partition favorably into aqueous vapor phases at low pressure but become mobile at pressure around 20 k bar [50]. CO_2 vapors tend to concentrate REE especially LREE.

Hydrothermal transport of REE was documented by many workers [51-55]. Limited experimental data suggest that REE $(Cl, F)^+_2$ may be the most stable complex at 25°C, 1 bar, in Cl—and F—rich solution [56-58] suggested that F-rich fluids facilitated REE mobility in the Cornubian granite by complexing Zr, thus destabilizing REE-bearing zircons. These data suggest an important role for F complexes in adition to CO_2 in mobilizing REE in low-pressure hydrothermal system. Mineyev (1963) summarized evidence for the importance of complexing in geochemical processes and found that high concentration of the REE, especially the HREE, are associated with high concentration of alkalis and volatiles. [59] studied the Kazakhstan massif, which had undergone a series of alteration processes with fluids showing considerable variations in PH. He found that the REE showed a sequence of evolution from LREE enriched near the center of the massif to HREE enriched at the periphery, with concomitant increase in the fluoride and alkali contents of the rock. [60] argued that very concentrated brines would be expected to become enriched in HREE and if precipitation occurs due to the mixing with less saline solutions, the resulting precipitates should also reflect this HREE-enrichment. Such changes have been observed in many hydrothermal systems [60].

According to the above discussion and available experimental work, the HREE enrichment in the Tawlah albite granite is largely controlled by the composition of the hydrothermal fluids (F-, Cl- or CO_2-enriched fluids), pH and fluid salinity. The metasomatic fluids involved during the formation of the Tawlah albitized granites were enriched in F-Cl and alkalies with high salinity. These metasomatic fluids caused albitization and concomitant precipitation of HREE and other rare metals (Nb, Ta, Zr and Y). The significant buildup in the HREE and the development of prominant Eu anomalies are the characteristic of sodium-metasomatized granites [61].

6. Conclusions

The data presented here led to the following concluding remarks:

1. The Jabal Tawlah is a late Neoproterozoic post-collision A-type granite pluton that intrudes island arc metavolcanosedimentary association in the Arabian Shield. Field observations indicate that the contacts between the albite granite and the country rocks are irregular, diffused and locally marked by silicification and abundant quartz veins, which affect both the country rocks and the granite.
2. The Jabal Tawlah granite consists of two petrographic varieties: i) quartz syenite, which occupies the central part of the granite mass and consists of microcline (up to 60%), albite, quartz and biotite in addition to minor accessory zircon, fluorite and opaque minerals, ii) albite granite that occupies the outer margin of the granite mass and consists of albite, quartz, microcline and abundant disseminations of accessory minerals (5-15%) represented by zircon, thorite, titanite, fluorite, apatite and many deep brown to black opaque grains.
3. The albite granite of Jabal Tawlah reveals a wide variation in major element composition (SiO_2 = 59.4 - 75.7%; Na_2O = 2.17 - 10.36%; K_2O = 0.15 - 10.18%; Al_2O_3 = 9.16 - 15.64%). The quartz syenite, on the other hand, shows a more homogenous and restricted composition than the albite granite. In addition, the specimens all have high Fe/Mg and total alkali contents, and low Ti, Mg, Ca, and P.
4. The albite granite of Jabal Tawlah is distinguished by its high concentration of Rb, Cs, Sn, Zn, Ta, Nb, Hf, Zr, Y, Th and HREE relative to the quartz syenite. The rare-metal enrichment in the Tawlah albite granite is largely controlled by hydrothermal fluids that post-date the intrusion of the granite mass. These metasomatic fluids caused albitization and concomitant precipitation of HREE and other rare metals (Nb, Ta, Zr and Y). The significant buildup in the HREE and the development of prominant Eu anomalies are characteristic of sodium-metasomatized granites.
5. Crystal-melt fractionation of feldspars and biotite is the dominant process that controls the evolution of these granites.

References

[1] Tischendorf, G. *Geochemical and Petrographic Characteristics of Silicic Magmatic Rocks Associated with Rare-element Mineralization.* In: M. Stemprok and I. Burnet (Eds.), "Metallization associated with acid magmatism." *Czechoslovakian Geol. Surv., Prague,* 2 (1977), 41-96.

[2] Loiselle, M.C. and Wones, D.R. "Characteristics and Origin of Anorogenic Granites." *Geol. Soc. Am. Abstr. Prog,* 11 (1979), 468.

[3] Collins, W.J.; Beams, S.D.; White, A.J.R. and Chappell, B.W. "Nature and Origin of A-type Granites with Particular Reference to Southeastern Australia." *Contrib. Mineral. Petrol.*, 80 (1982), 189-200.

[4] Pollard, P.J. "Geologic Characteristics and Genetic Problems Associated with the Development of Granite-hosted Deposits of Tantalum and Niobium." In: P. Moller, P. Cerny and F. Saupe (Eds.), *Lanthanides, Tantalum and Niobium*. Berlin: Springer, 1986, pp. 240–256.

[5] Cuney, M.; Marignac, C. and Weisbrod, A. "The Beauvoir Topaz–lepidolite–albite Granite (Massif Central, France): The Disseminated Magmatic Sn–Li–Ta–Nb–Be Mineralization." *Econ. Geol.*, 87 (1992), 1766–1794.

[6] Schwartz, M.O. "Geochemical Criteria for Distinguishing Magmatic and Metasomatic Albite-enrichment in Granitoids: Examples for the Ta-Li Granite Yichun (China) and the Sn-W Deposit Tikus (Indonesia)." *Mineral. Dep.*, 27 (1992), 101-108.

[7] Yin, L.; Pollard, P.J.; Hu, S. and Taylor, R.G. "Geologic and Geochemical Characteristics of the Yichun Ta–Nb–Li Deposit, Jiangxi Province, China." *Econ. Geol.*, 90 (1995), 577–585.

[8] Raimbault, L.; Cuney, M.; Azencott, C.; Duthou, J.L. and Joron, J.L. "Geochemical Evidence for a Multistage Magmatic Genesis of Ta–Sn–Li Mineralization in the Granite at Beauvoir, French Massif Central." *Econ. Geol.*, 90 (1995), 548–576

[9] Helba, H.; Trumbull, R.B.; Morteani, G.; Khalil, S.O. and Arslan, A. "Geochemical and Petrographic Studies of Ta Mineralization in the Nuweibi Albite Granite Complex, Eastern Desert, Egypt." *Mineral. Dep.*, 32 (1997), 164-179.

[10] Stoeser, D.B. "Distribution and Tectonic Setting of Plutonic Rocks of the Arabian Shield." *J. Afr. Earth Sci.*, 4 (1986), 21-46.

[11] Du Bary, E.A. "Specialized Granitoids in the Southeastern Arabian Shield: Case History of a Regional Assessment." *J. Afr. Earth Sci.*, 4 (1986), 169-176.

[12] Ramsay, C.R. "Specialized Felsic Plutonic Rocks of the Arabian Shield and Their Precursors." *J. Afr. Earth Sci.*, 4 (1986), 153-168.

[13] Ramsay, C.R.; Drysdall, A.R. and Clark, M.D. "Felsic Plutonic Rocks of the Midyan Region, Kingdom of Saudi Arabia: I. Distribution, Classification and Resource Potential." *J. Afr. Earth Sci.*, 4 (1986), 63-77.

[14] Clark, M. D. "Geology of Al-Bada Quadrangle, Sheet 28A, Kingdom of Saudi Arabia". *Saudi Arabian Deputy Ministry for Mineral Resources*, Open-File Report, 1987, [DGMR].

[15] Hedge, C. E. "Precambrian Geochronology of Part of Northwestern Saudi Arabia." *Saudi Arabian Dep. Min. Mineral Res.*, Open-File Report USGS-OF-04-31, (1984), 12 p.

[16] Hassanen, M.A. and Harraz, H.Z. "Geochemistry and Sr- and Nd-isotopic Study on Rare Metal-bearing Granitic Rocks, Central Eastern Desert, Egypt." *Precamb. Res.*, 80 (1996), 1-22.

[17] Hassanen, M.A. "Post-collision, A-type Granites of Homrit Waggat Complex, Egypt: Petrological and Geochemical Constraints on Its Origin." *Precamb. Res.*, 82 (1997), 211-236.

[18] Smith, J. V. *Feldspar Mineralogy*. Vol. 1, Berlin, New York, Heidelberg: Springer-Verlag, 1974.

[19] Allègre, C. J.; Hart, S. R. and Minster, J. F. "Chemical Structure and Evolution of the Mantle and Continents Determined by Inversion of Nd and Sr Isotopic Data, Numerical Experiments and Discussions." *Earth Planet. Sci. Lett.*, 37 (1983), 191-213.

[20] Jacobsen, S. B. and Wasserburg, G. J. "Sm-Nd Isotopic Evolution of Chondrites and Achondrites." *Earth Planet. Sci. Lett.*, 67 (1984), 137-150.

[21] Steiger, R. H. and Jager, E. "Subcommission on Geochronology: The Use of Decay Constants in Geo- and Cosmochronology." *Earth and Planet. Sci. Lett.*, 36 (1977), 359-362.

[22] DePaolo, D. J. "Trace Element and Isotopic Effects of Combined Wallrock Assimilation and Fractional Crystallization." *Earth Planet. Sci. Lett.*, 53 (1981), 189-202.

[23] Shand, S. J. *The Eruptive Rocks*. 1st ed., New York: John Wiley, 1927, 488 p.

[24] Batchelor, R. A. and Bowden, P. "Petrogenetic Interpretation of Granitoid Rock Series Using Multicationic Parameters." *Chem. Geol.*, 48 (1985), 43-55.

[25] Maniar, P.D. and Piccoli, P.M. "Tectonic Discrimination of Granitoids." *Geol Soc Am. Bull.*, 101 (1989), 635–643.

[26] Debon, F. and Lemmet, M. "Evolution of Mg/Fe Ratios in Late Variscan Plutonic Rocks from External Crystalline Massifs of the Alps (France, Italy, Switzerland)." *J. Petrol.*, 40 (1999), 1151-1185.

[27] Sum, S-S. and McDonough, W.E. "Chemical and Isotopic Systematics of Oceanic Basalts: Implications for Mantle Composition and Processes." In: A.D. Saunders and M.J. Norry (Eds.), *Magmatism in the Oceanic Basins*. London: Spec. Publ., 1989, pp. 313-345.

[28] Sun, S-S. "Chemical Composition and Origin of the Earth's Primitive Mantle." *Geochim. Cosmochim. Acta*, 46 (1982), 179-192.
[29] Whalen, J.B.; Currie, K.L. and Chappell, B.W. "A-type Granites: Geochemical Characteristics, Discrimination and Petrogenesis." *Contrib. Mineral. Petrol.*, 95 (1987), 407-419.
[30] Clemens, J.D.; Holloway, J.R. and White, A.J.R. "Origin of an A-type Granite: Experimental Constraints." *Am. Miner.*, 79 (1986), 71-86.
[31] Eby, G.N. "The A-type Granitoids: A Review of Their Occurrence and Chemical Characteristics and Speculations on Their Petrogenesis." *Lithos*, 26 (1990), 115-134.
[32] Eby, G.N. "Chemical Subdivisions of the A-type Granitoids: Petrogenesis and Tectonic Implications." *Geology*, 20 (1992), 641-644.
[33] Manning, D.A.C. "The Effect of Fluorine on Liquidus Phase Relationships in the System Qz-Ab-Or with Excess Water." *Contrib. Mineral. Petrol.*, 76 (1981), 206-215.
[34] Pearce, J.A.; Harris, N.B.W. and Tindle, A.G. "Trace Element Discrimination Diagrams for the Tectonic Interpretation of Granitic Rocks." *J. Petrol.*, 25 (1984), 956-983.
[35] Landenberger, B. and Collins, W.J. "Derivation of A-type Granites from Dehydrated Charnockitic Lower Crust: Evidence from the Chaelundi Complex Eastern Australia." *J. Petrol.*, 37 (1996), 145-170.
[36] King, P.L.; White, A.J.R.; Chappell, B.W. and Allen, M.C. "Characterization and Origin of Aluminous A-type Granites from the Lechlan Fold Belt Southeastern Australia." *J. Petrol.*, 38 (1997), 371-391.
[37] Küster, D. and Harms, U. "Post-collisional Potassic Granitoids from the Southern and Northwestern Parts of the Late Neoproterozoic East African Orogen: A Review." *Lithos*, 45 (1998), 177-195.
[38] Stern, R.J. and Gottfried, D. "Petrogenesis of Late Precambrian (575-600 Ma) Bimodal Suite in Northeast Africa." *Contrib. Mineral. Petrol.*, 92 (1986), 492-501.
[39] Turner, S.P.; Foden, J.D. and Morrison, R.S. "Derivation of Some A-type Granites by Fractionation of Basaltic Magma: An Example from the Padthaway Ridge, South Australia." *Lithos*, 28 (1992), 151-179.
[40] Beyth, M.; Stern, R.J.; Altherr, R. and Kroner, A. "The Late Precambrian Timna Igneous Complex, Southern Israel: Evidence for Comagmatic-type Sanukitoid Monzodiorite and Alkali Granite Magma." *Lithos*, 31 (1994), 103-124.
[41] Whalen, J.B.; Jenner, G.A.; Longstaffe, F.J.; Robert, F. and Gariépy, C. "Geochemical and Isotopic (O, Nd, Pb and Sr) Constraints on A-type Granite Petrogenesis Based on the Topsails Igneous Suite Newfoundland Appalachians." *J. Petrol.*, 37 (1996), 1463-1489.
[42] Kerr, A. and Fryer, B.J. "Nd Isotope Evidence for Crust-mantle Interaction in the Generation of A-type Granitoid Suites in Labrador Canada." *Chem. Geol.*, 104 (1993), 39-60.
[43] Gettings, M.E.; Blank, H.R.; Mooney, W.D. and Healey, J.H. "Crustal Structure of Southwestern Saudi Arabia." *J. Geoph. Res.*, 91 (1986), 6491-6512.
[44] McGuire, A.V. and Stern, R.J. "Granulite Xenoliths from Western Saudi Arabia: The Lower Crust of the Late Precambrian Arabian-Nubian Shield." *Contrib. Mineral. Petrol.*, 114 (1993), 395-408.
[45] Wolf, M.B. and Wyllie, P.J. "Dehydration-melting of Amphibolites at 10 kbar: The Effects of Temperature and Time." *Contrib. Mineral. Petrol.*, 115 (1994), 369-383.
[46] Beard, J.S. and Lofgren, G.E. "Dehydration Melting and Water-saturated Melting of Basaltic and Andesitic Greenstones and Amphibolites at 1, 3 and 6.9 kbar." *J. Petrol.*, 32 (1991), 365-402.
[47] Taylor, R.P.; Strong, D.F. and Freyer, B.J. "Volatile Control of Contrasting Trace Element Distributions in Peralkaline Granitic and Volcanic Rocks." *Contrib. Mineral. Petrol.*, 77 (1981), 267-271.
[48] London, D. "Internal Differentiation of Rare Element Pegmatites: Effects of Boron, Phoshphorus, and Fluorine." *Geochim. Cosmochim Acta*, 51 (1987), 403-420.
[49] Henderson, P. *Rare Earth Element Geochemistry*. New York: Elsevier, 1984, 510 p.
[50] Wendlandt, R. F. and Harrison, W. J. "Rare Earth Partitioning between Immiscible Carbonate and Silicate Liquids and CO_2 Vapor: Results and Implications for the Formation of Light Rare Earth-enriched Rocks." *Contrib. Mineral. Petrol.*, 69 (1979), 409-419.
[51] Dostal, J.; Strong, D. F. and Jamieson, R. A. "Trace Element Mobility in the Mylonite Zone within the Ophiolite Aureole, St. Anthony Complex, Newfoundland." *Earth Planet. Sci. Letters*, 49 (1980), 188-192.
[52] Campell, I. H.; Lesher, C. M.; Coad, P.; Franklin, J. M.; Gorton, M. P. and Thurston, P. C. "Rare Earth Elements Mobility in Alteration Pipes below Massive Cu-Zn Sulfide Deposits." *Chem. Geol.*, 45 (1984), 181-202.
[53] Elders, W. A. "Data on Solid Samples from Five Wells in the Salton Sea Geothermal Field and Representative Surface Samples." *Riverside, Univ. California, Rept. IGPP*, 85-12 (1985), 20-23.

[54] Maas, R.; McCulloch, M. T.; Campbell, I. H. and Page, R. W. "Sm-Nd Isotope Systematics in Uranium-rare Earth Element Mineralization at the Mary Kathleen Uranium Mine, Queensland." *Econ. Geol.*, 82 (1987), 1805-1826.

[55] Oreskes, N. and Einaudi, M. T. "Origin of Rare Earth-enriched Hematite Breccias at the Olympic Dam Cu-U-Au-ag Deposit, Roxby Downs, South Australia." *Econ. Geol.*, 85 (1990), 1-28.

[56] Sillen, L.C. and Martell, A. E. "Stability Constants of Metal-ion Complexes, London." *Chem. Soc. Spec. Pub.*, 17 (1971), 754 p.

[57] Humphris, S. "Mobility of Rare Earth Elements in the Crust." In: P. Hendrson (Ed.), *Rare Earth Element Geochemistry*. Amsterdam: Elsevier, 1984, pp. 317-340.

[58] Alderton, D. H. M.; Pearce, J. A. and Potts, P. J. "Rare Earth Element Mobility during Granite Alteration: Evidence from Southwest England." *Earth Planet. Sci. Letters*, 49 (1980), 149-165.

[59] Mineyev, D. A. "Geochemical Differentiation of Rare Earths." *Geochemistry*, 12 (1963), 1129-1149.

[60] Moller, P.; Morteani, G.; Hoefs, J. and Parekh, P. P. "The Origin of the Ore-bearing Solution in Pb-Zn Veins of the Western Harz, Germany, as Deduced from Rare-earth Element and Isotope Distributions in Calcite." *Chem. Geol.*, 26 (1979), 197-215.

[61] Bowden, P.; Bennett, J. N.; Whitley, J. E. and Moyes, A. B. "Rare Earths in Nigerian Mesozoic Granites and Related Rocks." In: L.H. Ahrens (Ed.), *Origin and Distribution of the Elements*. Pergamon Press, 1979, pp. 479-491.

نشأة الجرانيت الألبيتي المتمعدن الحامل للفلزات النادرة – مثال من جبل طاولة التابع للنيوبروتيروزوي المتأخر في شمال الدرع العربي بالمملكة العربية السعودية

طلال بن مصطفى قاضي

قسم الثروة المعدنية والصخور، كلية علوم الأرض، جامعة الملك عبد العزيز، جدة، المملكة العربية السعودية

(قدم للنشر في ١٤٢٧/٤/٢٣هـ؛ وقبل للنشر في ١٤٢٧/٨/١٩هـ)

ملخص البحث. ينتمي محقون جبل طاولة، والذي يقع في الجزء الشمالي الغربي من الدرع العربي، إلى الجرانيتات القلوية من نوع A التابعة لفترة ما بعد التجبل للنيوبروتيروزوي المتأخر في المملكة، حيث تم تقدير عمره بحوالي ٦٠٧ ملايين سنة. وقد تداخل هذا المحقون في صخور بركانية-رسوبية ذات خصائص قوس جزيري حيث لوحظ أثناء الدراسة الحقلية أن الحد الفاصل بين النوعين من الصخور غير منتظم، ويتميز في بعض المناطق بوجود العديد من عروق المرو وكذا بعض التغيرات السيليسية والتي أثرت على صخور المحقون وصخور القوس الجزيري. وبناء على الدراسات المجهرية فقد أمكن التعرف على نوعين أساسيين من صخور الجرانيت في جبل طاولة. النوع الأول هو سيانيت الكوارتز والذي يحتل الجزء الأوسط من المحقون ويتكون أساسا من الميكروكلين (حوالي ٦٠٪) والألبيت والكوارتز والبيوتيت بالإضافة إلى الزركون والفلوريت والهيماتيت كمعادن مساعدة. أما النوع الثاني فهو يمثل الجزء الأكبر من المحقون حيث يحتل الحواف الخارجية ويتكون من الألبيت والكوارتز والميكروكلين والكثير من المعادن المساعدة والمعادن الفلزية والتي تصل نسبتها إلى ١٥٪ وممثلة بمعادن الزركون والثوريت والتيتانيت والفلوريت والأباتيت والكولمبيت والتابيوليت.

وأشارت الدراسات الجيوكيميائية وكذا نظائر النيوديميوم (إبسيلون نيوديميوم = – +٤.٢ – +٥.٩) إلى أن الصهير الأصلي لجرانيت جبل طاولة نتج بواسطة عملية انصهار جزئي لقشرة أرضية حديثة، ثم أتبع ذلك عمليات تبلور تجزيئي، كما أشارت الدراسات الجيوكيميائية أيضًا إلى عدم وجود تجانس كبير في محتوى العناصر الرئيسية والشحيحة بين النوعيات المختلفة من الجرانيت المكون لجبل طاولة. فقد تميز سيانيت الكوارتز بأنه فائض القلوية وبأنه متجانس نسبيًا وله محتوى عالي من القلويات ونسبة الحديد/الماغنيسيوم ومحتوى منخفض من